



ARTICLE

Suppression of monosodium urate crystal-induced inflammation by inhibiting TGF- β -activated kinase 1-dependent signaling: role of the ubiquitin proteasome system

Anil K. Singh¹, Mahamudul Haque¹, Kayla O'Sullivan¹, Mukesh Chourasia², Madhu M. Ouseph³ and Salahuddin Ahmed^{1,4}

Monosodium urate (MSU) crystals activate inflammatory pathways that overlap with interleukin-1 β (IL-1 β) signaling. However, the post-translational mechanisms involved and the role of signaling proteins in this activation are unknown. In the present study, we investigated the intracellular signaling mechanisms involved in MSU-induced activation of THP-1 macrophages and human nondiseased synovial fibroblasts (NLSFs) and the in vivo efficacy of an inhibitor of tumor growth factor- β (TGF- β)-activated kinase 1 (TAK1), 5Z-7-oxozeaenol, in MSU-induced paw inflammation in C57BL/6 mice. THP-1 macrophage activation with MSU crystals (25–200 μ g/ml) resulted in the rapid and sustained phosphorylation of interleukin-1 receptor-activated kinase 1 (IRAK1 Thr²⁰⁹) and TAK1 (Thr^{184/187}) and their association with the E3 ubiquitin ligase TRAF6. At the cellular level, MSU inhibited the deubiquitinases A20 and UCHL2 and increased 20s proteasomal activity, leading to a global decrease in K⁶³-linked ubiquitination and increase in K⁴⁸-linked ubiquitination in THP-1 macrophages. While MSU did not stimulate cytokine production in NLSFs, it significantly amplified IL-1 β -induced IL-6, IL-8, and ENA-78/CXCL5 production. Docking studies and MD simulations followed by TAK1 in vitro kinase assays revealed that uric acid molecules are capable of arresting TAK1 in an active-state conformation, resulting in sustained TAK1 kinase activation. Importantly, MSU-induced proinflammatory cytokine production was completely inhibited by 5Z-7-oxozeaenol but not IRAK1/4 or TRAF6 inhibitors. Administration of 5Z-7-oxozeaenol (5 or 15 mg/kg; orally) significantly inhibited MSU-induced paw inflammation in C57BL/6 mice. Our study identifies a novel post-translational mechanism of TAK1 activation by MSU and suggests the therapeutic potential of TAK1 in regulating MSU-induced inflammation.

Keywords: Monosodium urate crystals; Gout; TAK1; Ubiquitination; 5Z-7-oxozeaenol

Cellular & Molecular Immunology (2021) 18:162–170; <https://doi.org/10.1038/s41423-019-0284-3>

INTRODUCTION

Gout is characterized by painful and progressive attacks of acute inflammation due to the deposition of monosodium urate (MSU) crystals in joints and periarticular tissues. Current therapies for the management of gout include uric acid-lowering therapies (ULTs), such as allopurinol or febuxostat, and colchicine, which inhibits inflammation.¹ Although the prevalence of gout is increasing, the management strategies for gout remain suboptimal.² This discrepancy is partly attributed to a limited understanding of the underlying mechanisms exploited by MSU crystals to induce gouty inflammation and tissue destruction. Studies suggest that MSU utilizes the Toll-like/interleukin-1 β (IL-1 β) receptor (TIR) signaling system, in which adaptor proteins such as Myd88 and IL-1R1 are essential to trigger an acute inflammatory response to IL-1 β .^{3,4} Studies also suggest that MSU crystals activate the NALP3 inflammasome to expedite IL-1 β processing.⁵

The centrality of IL-1 β in mediating MSU-induced acute inflammation has triggered interest in the clinical testing of IL-1 β inhibitors.^{6,7} While the short-term use of these IL-1 inhibitors seems promising, problems such as efficacy limited to a subset of

the patient population, increased risk of infection with long-term use, and socioeconomic challenges associated with delivery not observed with conventional medications emphasize the need for novel therapeutic approaches.² Moreover, the underlying mechanism through which MSU crystals activate resident cells in the joints such as synovial fibroblasts remains unclear.

Post-translational modifications (PTMs) play an essential role in relaying cellular signals initiated by TLRs, cytokines, or growth factors.⁸ One such PTM, ubiquitination, plays an important role in the TLR, IL-1 β , and tumor necrosis factor- α (TNF- α) signaling pathways by either stabilizing signaling proteins via K⁶³-linked ubiquitin chains or initiating proteasomal degradation by tagging proteins with K⁴⁸-linked ubiquitin chains.⁹ The ubiquitination process is mediated by E3 ubiquitin ligases such as TNF receptor-associated factor (TRAF2 or TRAF6) that receive signals from adaptor proteins proximal to IL-1 or TNF receptors to activate the downstream nuclear factor- κ B (NF- κ B) and mitogen-activated protein kinase (MAPK) pathways.^{8,9} The central position of TGF- β -activated kinase 1 (TAK1) in the cytokine and TLR signaling pathways makes it an attractive therapeutic target.^{10–12} Whether

¹Department of Pharmaceutical Sciences, Washington State University College of Pharmacy, Spokane, WA, USA; ²Center for Computational Biology and Bioinformatics, Amity Institute of Biotechnology, Amity University, Noida, Uttar Pradesh, India; ³Department of Pathology, Stanford University School of Medicine, Stanford, CA, USA and ⁴Division of Rheumatology, University of Washington School of Medicine, Seattle, WA, USA
Correspondence: Salahuddin Ahmed (salah.ahmed@wsu.edu)

Received: 1 March 2019 Accepted: 19 August 2019

Published online: 11 September 2019

MSU crystals, which are known to bind IL-1R1 and Myd88, utilize PTMs to activate IL-1 β inflammatory signaling is not known.

MATERIALS AND METHODS

Antibodies and reagents

Please see detailed information in the Supplementary Materials and methods section.

Cell culture and stimulation

Human monocytic leukemia (THP-1) cells were maintained in RPMI-1640 culture medium with 10% fetal bovine serum and antibiotics. For the experiments, THP-1 cells were differentiated into macrophages with phorbol 12-myristate 13-acetate (250 ng/ml) for 3 h by a method described previously,^{13,14} followed by medium replacement with fresh Opti-MEM overnight. The next day, differentiated THP-1 cells (2×10^6) were stimulated with different concentrations (25–200 $\mu\text{g/ml}$) of endotoxin-free MSU crystals (Cat#: Tlr1-25; Invivogen) for different time periods. THP-1 macrophages (1×10^4 per well) were seeded in 96-well plates and stimulated with MSU (25–200 $\mu\text{g/ml}$) for 24 h to evaluate the effect of MSU on cell viability by a previously described method.¹⁵

For inhibitor experiments, THP-1 macrophages were pretreated with interleukin-1 receptor-activated kinase 1 (IRAK1) inhibitors [N-(2-morpholinylethyl)-2-(3-nitrobenzoylamido)-benzimidazole; 0.5–10 μM], TAK1 [5Z-7-oxozeaenol; 0.05–5 μM], TRAF6 inhibitor peptide [10–20 μM], or control peptide [10–20 μM] for 2 h in fresh Opti-MEM, followed by MSU (100 $\mu\text{g/ml}$) stimulation for either 30 min for Western blotting or 24 h to measure released cytokines.

Primary human synovial fibroblasts from nondiseased (NLSFs) donors and donors with rheumatoid arthritis (RASFs) were obtained from synovial tissues under an Institutional Review Board-approved protocol and cultured using a previously described method.¹⁶ Confluent cells (2×10^6 in 35 mm dishes) were serum-starved overnight and stimulated with different concentrations (25–100 $\mu\text{g/ml}$) of endotoxin-free MSU for 30 min to study the signaling mechanisms or 24 h to determine the effect of MSU on protein release. MSU (25–100 $\mu\text{g/ml}$) was also added to the cells in the presence of a low concentration of IL-1 β (1 ng/ml) for 24 h to determine their combined effect on cytokine production.

Cytokine measurements

Individual cytokine levels in the conditioned media were measured using DuoSet ELISA (enzyme-linked immunosorbent assay) kits for human IL-1 β , TNF- α , IL-8, and monocyte chemoattractant protein-1 (MCP-1) (R&D Systems, MN).

Western blotting

Western blotting was performed as previously described.^{12,17} Specific details are provided in the Supplementary Material and methods section.

Immunoprecipitation assay

THP-1 cells (1×10^7) in 100 mm dishes were starved overnight with Opti-MEM, pretreated with 5Z-7-oxozeaenol for 2 h, and finally stimulated with MSU (100 $\mu\text{g/ml}$) for 30 min. Immunoprecipitation using mouse monoclonal antibodies against FK2, TRAF6, and TAK1 at the specified dilutions was performed as previously described.¹²

In vitro TAK1 kinase assay

An in vitro TAK1 kinase assay was performed using a TAK1/TAB1 fusion protein. Specific details of TAK1/TAB1 fusion protein expression, purification, and utilization in the kinase assay are provided in the Supplementary Materials and methods section.

Small interfering RNA (siRNA) method

Predesigned small interfering RNA (siRNA) sequences for IRAK1 (SASI_Hs01_00017884 and SASI_Hs02_00307425), TRAF6

(SASI_Hs01_00116399 and SASI_Hs01_00116390), IL-1 β (SASI_Hs01_00028205 and SASI_Hs01_00028206), and TAK1 (SASI_Hs01_00166582, SASI_Hs02_00365229, and SASI_Hs02_00365227) were purchased from Sigma MISSION. THP-1 macrophages were transfected with 120 pmol of scrambled (SIC001) or targeted siRNAs with Lipofectamine 2000 for 48 h using a recently described method.¹⁸ After 48 h of transfection, cells were serum-starved overnight prior to MSU simulation for 24 h.

Molecular modeling studies and ligand preparation

All computational studies were performed using different modules of Schrodinger suite 15.3 as described previously.^{12,19} A detailed procedure is provided in the Supplementary Materials and methods section.

Human peripheral blood mononuclear cell-derived macrophage culture

Human peripheral blood mononuclear cells (PBMCs) obtained from a commercial source (Zen-Bio, Inc., Research Triangle, NC, USA) were differentiated into macrophages by a method described earlier.²⁰ Experimental details are provided in the Supplementary Material and Methods section.

Animal experimentation

All animal experiments were approved by the Washington State University IACUC committee (protocol approval number: 04775). We chose C57BL/6 male mice since they are susceptible to the development of paw inflammation when injected with a suspension of MSU crystals (0.5 mg, Invivogen) in 20 μl of endotoxin-free phosphate-buffered saline using 27-gauge syringes (Cat#: 705SN, Hamilton, NY) as described recently.²¹ A detailed procedure is provided in the Supplementary Materials and Methods section. Paw circumference was calculated using a previously described method.¹⁷

Histological analysis of ankles

Fresh-frozen sections (6 μm) of joints from experimental mice were stained with hematoxylin & eosin (H&E) and processed as previously described.¹⁷ For an objective evaluation of synovitis and inflammation, slides were analyzed by a pathologist for the following parameters: polymorphonuclear inflammation, immune cell infiltration (lymphocytes, plasma cells, and macrophages), neovascularization, and fibrosis (Supplementary Table 1), as described in our recent study.²²

Statistical analysis

The Student's *t* test was performed to calculate the statistical significance of differences between the means of different protein variables obtained from in vivo findings. *P* values <0.05 (two-tailed) indicated significance.

RESULTS

MSU crystals induce the autophosphorylation of IL-1 β signaling proteins

THP-1 macrophages treated with MSU (25–200 $\mu\text{g/ml}$) for 30 min showed a gradual increase in the autophosphorylation of IRAK1 (Thr³⁸⁷) that peaked with an MSU concentration of $\sim 100 \mu\text{g/ml}$ (Fig. 1a). In contrast to canonical IL-1 β or TLR signaling, in which IRAK1 degrades, MSU induced the activation of p-IRAK1 (Thr³⁸⁷). To our surprise, we observed the increased phosphorylation of TAK1 at the Thr^{184/187} position, which is essential for its kinase activation.²³ Furthermore, MSU induced a time-dependent increase in the phosphorylation of IRAK1 at Thr^{209/387} and TAK1 at Thr^{184/187} in THP-1 macrophages that peaked at ~ 60 min without affecting their viability (Fig. 1b; densitometric analysis in Supplementary Fig. S1A–C and viability data in Fig. S2A). To verify that this early effect is not governed by released IL-1 β , we carried

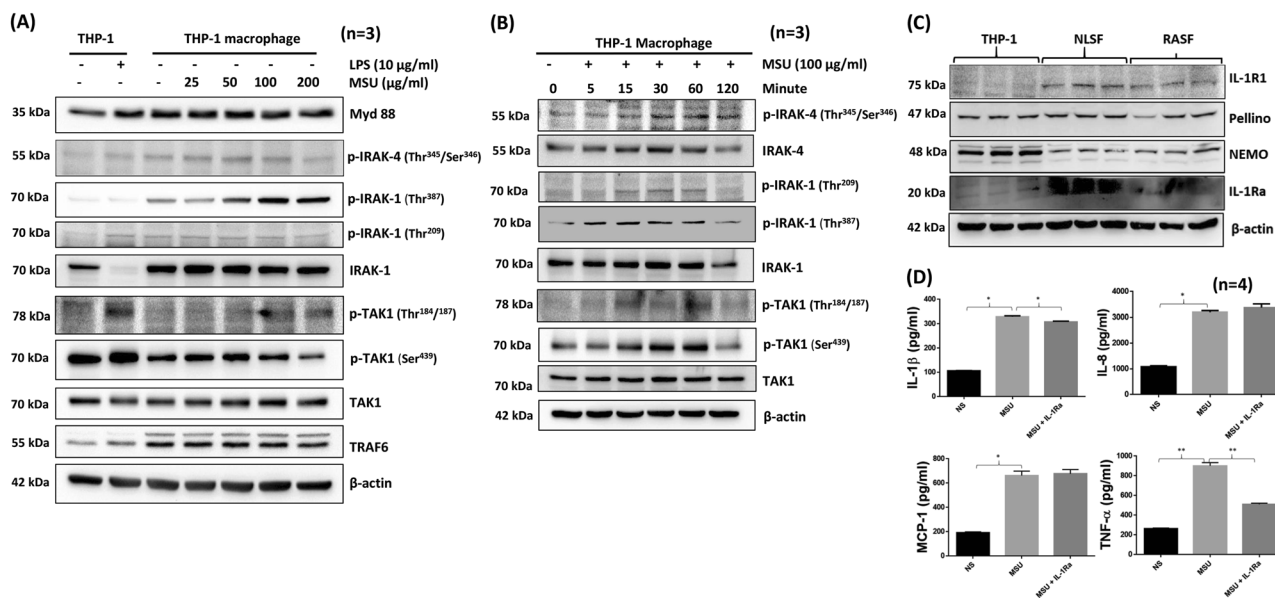


Fig. 1 MSU activates signaling pathways in THP-1 macrophages similar to IL-1 β -mediated signaling. **a** THP-1 macrophages (2×10^6 /well) in 6-well plates were stimulated with LPS (10 μ g/ml) or MSU (25–200 μ g/ml) for 30 min. Cell lysates prepared from these samples were analyzed for phosphorylated and unphosphorylated proteins. **b** Time-dependent activation of signaling proteins in THP-1 macrophages stimulated with MSU (100 μ g/ml) for 0–120 min. **c** THP-1 macrophages, >85% confluent NLSFs or RASFs in 6-well plates were given serum-free medium overnight. Cell lysates were prepared the next day to study the constitutive expression levels of the signaling proteins IL-1R1, Pellino, NEMO, and IL-1Ra. Cell viability was evaluated using an MTT-based cell viability assay, and the data are shown as the percentage of the unstimulated control. **d** THP-1 macrophages (2×10^6 /well) in six-well plates were pretreated with recombinant human IL-1Ra (500 ng/ml), followed by MSU (100 μ g/ml) stimulation for 24 h. Conditioned media were collected at different time points and used to determine IL-1 β production. Representative blots and the quantitative results (mean \pm SEM) from three independent experiments. * $p < 0.05$ or ** $p < 0.01$ *

out different experimental approaches. First, we activated undifferentiated THP-1 monocytes with MSU for 30 min and observed by Western blot analysis that MSU can effectively induce the phosphorylation of IRAK1 (Thr³⁸⁷) and TAK1 (Thr^{184/187}) (Fig. S2B) in monocytic cells that do not produce IL-1 β (data not shown). Second, we evaluated the temporal production of IL- β and TNF- α in differentiated THP-1 macrophages treated with MSU (100 μ g/ml). Our results rule out the role of IL-1 β in TAK1 or IRAK1 activation since MSU induced significant and detectable levels of IL-1 β or TNF- α as early as 6 h (Fig. S2C).

To further rule out any canonical IL-1 β signaling by MSU, we determined the expression levels the IL-1R1, Pellino, NEMO, and IL-1Ra (an IL-1R antagonist) proteins in THP-1 macrophages and compared them to their expression levels in NLSFs and RASFs. Western blot analysis showed that THP-1 macrophages express no or negligible levels of IL-1R1 compared to those in NLSFs and RASFs; however, THP-1 macrophages expressed the Pellino and NEMO proteins at levels comparable to those observed in NLSFs and RASFs (Fig. 1c). To exclude the possible role of IL-1 β in the MSU-induced activation of signaling kinases, we treated THP-1 macrophages with IL-1 β or negative control (NC) siRNA prior to MSU (100 μ g/ml) stimulation for 24 h. Western blotting showed that IL-1 β knockdown had no effect on the ability of MSU to induce TAK1 activation (Fig. S3A). In addition, evaluation of the conditioned media from the same treated samples showed that IL-1 β siRNA significantly inhibited IL-1 β production, but had no effect on MSU-induced TNF- α production (Fig. S3B, C). Furthermore, THP-1 macrophages pretreated with exogenous IL-1Ra (500 ng/ml) showed no marked inhibition of MSU-induced IL-1 β , MCP-1, and IL-8 production, but a modestly reduction in TNF- α production (Fig. 1d), suggesting that MSU-induced signaling activation is independent of IL-1R or synthesized IL-1 β .

MSU activates primary human macrophages and synovial fibroblasts and facilitates cytokine production

To extend our observations of IL-1 β signaling activation in THP-1 macrophages to primary human cells, we stimulated human PBMC-derived macrophages with MSU (50–200 μ g/ml) for 30 min. Western blot analysis of lysates showed that MSU activated the phosphorylation of IRAK1 (Thr³⁸⁷) and TAK1 (Thr^{184/187}) in a dose-dependent manner (Fig. 2a). To understand the detrimental effects of MSU crystals on resident nonhematopoietic cells, we treated primary human NLSFs with MSU (25–100 μ g/ml) for 30 min and evaluated signaling pathways (Fig. 2). MSU induced the phosphorylation of IRAK1 (Thr²⁰⁹ and Thr³⁸⁷), and phosphorylated IRAK1 levels were comparable to those following activation by IL-1 β (Fig. 2b; Fig. S4A). However, the MSU-induced activation of TRAF6, TAK1 (Thr^{184/187}), TAK1 (Ser⁴³⁹), and TAB2 (Ser³⁷²) was strikingly different from the canonical activation mechanism driven by IL-1 β in human SFs.¹² To gain further insight into this difference, we treated NLSFs with a low dose of IL-1 β (1 ng/ml) and/or MSU (25–100 μ g/ml) for 24 h (Fig. 2c–f). Evaluation of released inflammatory proteins in the conditioned media showed that MSU alone had no effect on their induction (Fig. 2c); however, MSU further significantly enhanced the IL-1 β -induced production of IL-6, IL-8, and ENA-78/CXCL5 (Fig. 2c–f; $p < 0.05$, $p < 0.01$).

MSU exploits the protein ubiquitin system to relay IL-1 β -like signaling

THP-1 macrophages treated with different concentrations of MSU for 4 h showed a concentration-dependent increase in K⁴⁸-linked ubiquitination and concomitant decrease in K⁶³-linked ubiquitination, even at the lowest MSU concentration of 25 μ g/ml (Fig. 3a). We extended our studies to primary human macrophages and observed that treated with MSU (25–200 μ g/ml) for 24 h reduced K⁶³-linked ubiquitination in these cells as well (Fig. S4B). To

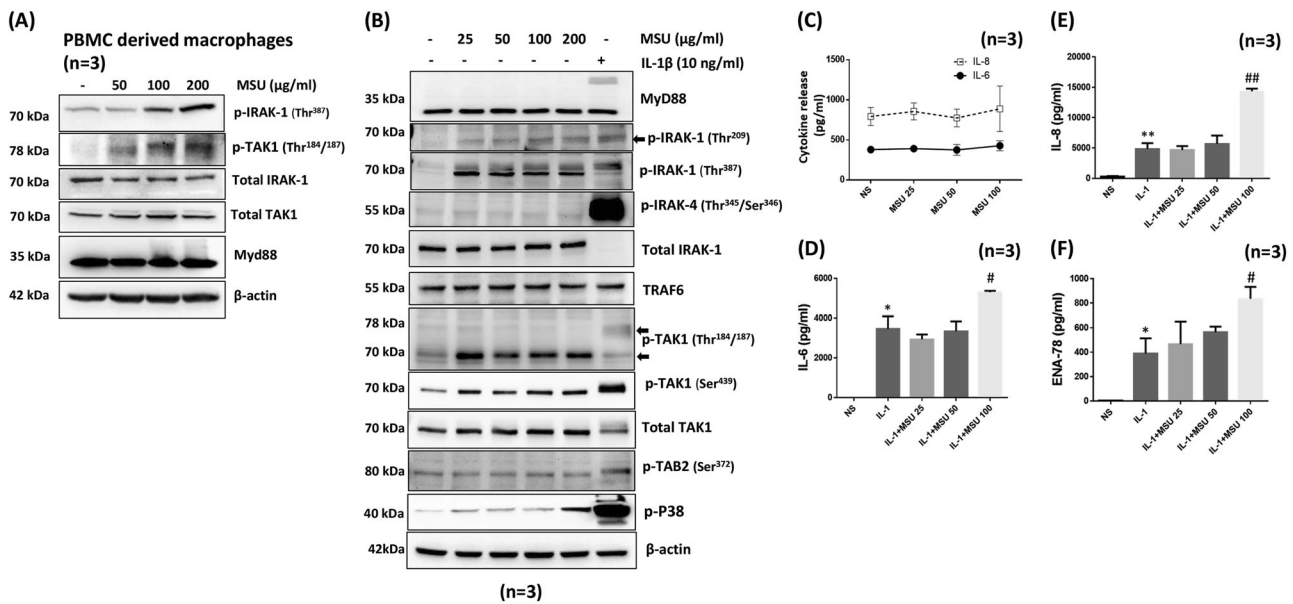


Fig. 2 MSU activates IL-1 β signaling proteins in primary human macrophages and coordinates with IL-1 β to induce cytokine production in primary human synovial fibroblasts. **a** Primary PBMC-derived human macrophages (2×10^6 /well) in six-well plates were stimulated with MSU (100 μ g/ml) for 30 min. Cell lysates were prepared to detect MyD88 and phosphorylated and total IRAK1 and TAK1. **b** Human NLSFs were treated with MSU (25–200 μ g/ml) or IL-1 β (10 ng/ml) for 30 min. Cell lysates were prepared to study activation of the signaling proteins MyD88, IRAK1, TRAF6, TAK1, and TAB2. **c–f** Human NLSFs were stimulated with MSU (25–100 μ g/ml) for 24 h. Conditioned media were collected and further utilized to quantitate IL-6 and IL-8 production. **c–f** Human NLSFs were treated with IL-1 β (1 ng/ml) alone or with MSU (25–100 μ g/ml) for 24 h, and the conditioned media were collected and used for the estimation of IL-6, IL-8, and ENA-78 production. The results shown in **b–f** were obtained from the experiment on NLSFs obtained from three different donors and are presented as the mean \pm SEM. * $p < 0.05$ or ** $p < 0.01$ vs. NS (not significant); # $p < 0.05$ or ## $p < 0.01$ vs. IL-1 β

confirm the generality of this effect of MSU, we treated human NLSFs with varying concentrations of MSU and observed that MSU is indeed able to activate K⁴⁸-linked ubiquitination in human NLSFs, with a modest concentration-dependent decrease in K⁶³-linked ubiquitination (Fig. 3b). We evaluated the impact of MSU (25–100 μ g/ml) on deubiquitinases in THP-1 macrophages and found that MSU inhibited the expression of the deubiquitinases A20 and UCHL2, but increased 26s proteasomal subunit PSMD13 expression in a dose-dependent manner (Fig. 3c; $p < 0.05$, densitometric analysis). These findings suggest that MSU can accelerate proteasome activity in THP-1 macrophages to induce inflammatory mediators. To confirm this finding, the results of an in vitro kinase assay showed that MSU at a concentration as low as 25 μ g/ml significantly increased proteasome activity by more than 25% and that this effect plateaued at up to 100 μ g/ml MSU (Fig. 3d).

TAK1 inhibition suppresses MSU-induced cytokine production
To understand the importance of IRAK1/4, TRAF6, and TAK1 in MSU-induced inflammation, we pretreated THP-1 macrophages with chemical inhibitors of IRAK1/4 or TAK1 and a peptide inhibitor of TRAF6, followed by MSU (100 μ g/ml) stimulation for 24 h (Fig. 4). Our ELISA results showed that the IRAK1/4 inhibitor had no significant inhibitory effect on MSU-induced TNF- α , IL-1 β , and IL-8 production, whereas 5Z-7-oxozeaenol completely inhibited the ability of MSU to induce expression of these cytokines and chemokines, suggesting the critical role of TAK1 in MSU-induced inflammation (Fig. 4a–d). We further confirmed these findings using siRNA targeting IRAK1, TRAF6, and TAK1. Our ELISA results showed that IRAK1, TRAF6, and TAK1 siRNA successfully inhibited MSU-induced IL-1 β and TNF- α production in THP-1 macrophages, but had no effect on MCP-1 and IL-8 production (Fig. 5A, B; $p < 0.05$). While these results partly confirmed those of inhibitor experiments, they also suggested that the use of siRNA to study the role of kinases does not provide conclusive results.

5Z-7-oxozeaenol modulates MSU-induced IL-1 β expression and ubiquitination

To understand the impact of the TAK1 inhibitor 5Z-7-oxozeaenol on IL-1 β production, we stimulated THP-1 macrophages with MSU for 30 min with or without 5Z-7-oxozeaenol pretreatment. Western blot analysis showed that MSU induced both the proform and mature form of IL-1 β (Fig. 4e). Interestingly, pretreatment with 5Z-7-oxozeaenol inhibited both constitutive and MSU-induced IL-1 β expression. 5Z-7-oxozeaenol pretreatment also downregulated IL-1 β maturation, as confirmed by reduced expression of a cleaved IL-1 β (Asp¹¹⁶) fragment (Fig. 4e), which was almost completely inhibited by 4 h of MSU stimulation (Fig. 4f). To determine whether this effect is due to proteasomal degradation, we treated THP-1 macrophages with 5Z-7-oxozeaenol in the presence of the proteasome inhibitor MG132 (10 μ M). MG132 pretreatment rescued 5Z-7-oxozeaenol-induced pro-IL-1 β protein degradation (Fig. 4g). Furthermore, our results in primary human macrophages showed that pretreatment with 5Z-7-oxozeaenol had no inhibitory effect on the phosphorylation of IRAK1 (Thr³⁸⁷), but markedly suppressed pro-IL-1 β expression (Fig. 4h). This novel finding suggests that TAK1 plays an important role in the stability of IL-1 β and that TAK1 inhibitors limit the role of mature or released IL-1 β by reducing pro-IL-1 β expression.

MSU crystals activate TAK1 kinase activity

MSU crystals in solution exist as tautomeric urate forms,²⁴ and these forms are equally capable of inducing IL-1 β production.²⁵ To determine whether soluble uric acid molecules can bind with TAK1 and induce its kinase activity, we simulated the placement of six molecules of uric acid in and around the active site of TAK1 in a TAK1-TAB1 fusion protein using Glide and submitted the final docked complex for molecular dynamics (MD) simulation. Up to four molecules of uric acid were found to occupy the active site of the TAK1-TAB1 protein without causing any significant changes in the secondary structure of the TAK1 protein (Fig. 5a, b; Fig. 5A–D).

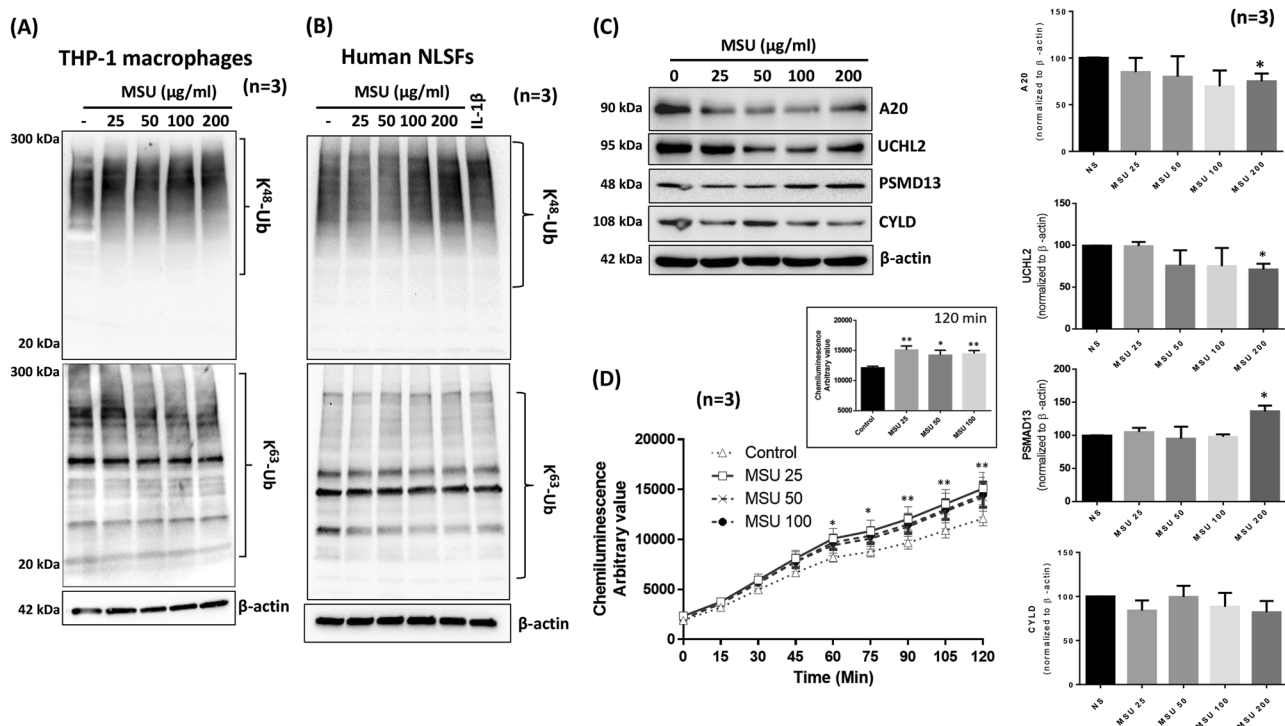


Fig. 3 MSU engages the ubiquitin proteasome system to facilitate signaling in THP-1 macrophages and human NLSFs. **a** THP-1 macrophages were stimulated with MSU (0–200 µg/ml) for 4 h, and cell lysates were probed for K⁴⁸- and K⁶³-linked ubiquitinated proteins. **b** Human NLSFs were treated with MSU (0–200 µg/ml) for 4 h, and cell lysates were probed for K⁴⁸- and K⁶³-linked ubiquitinated proteins. **c** Cell lysates from THP-1 macrophages treated with MSU (0–200 µg/ml) were probed for the deubiquitinases A20, CYLD, and UCHL2 and the 26S proteasome subunit PSMD13. Densitometric analysis of Western blots for A20, CYLD, UCHL2, and PSMD13 was performed, and protein intensities were normalized to β-actin intensities. The values represent the mean ± SEM of values obtained from three independent experiments for each protein. **d** The effect of MSU (25–100 µg/ml) on 20S proteasome activity was studied using an in vitro assay from a commercial source (Cayman Chemicals). An inset graph shows the increase in 20S proteasome activity induced by MSU (25–100 µg/ml) after 120 min. The values presented in the graph are the mean ± SEM of each sample run in triplicate. **p* < 0.05 or ***p* < 0.01 for NS (not significant) vs. MSU treatment

Furthermore, the phosphorylation loop of TAK1, which is far from the binding pocket, is stabilized by the binding of a uric acid molecule in the active site, thereby stabilizing the active conformation of TAK1 or delaying its dephosphorylation. A closer look at the interaction demonstrates the stable binding of one uric acid molecule in the binding pocket through the formation of H-bonds with V42, R44, E105, and the side chain of D175 (Fig. 5b), which is stabilized by hydrophobic interactions with the side chains of V50, M104, and L163. This site is proximal to the C174 site, which is occupied by 5Z-7-oxozeaenol through covalent bonds, causing the irreversible inhibition of TAK1 kinase activity.²³ The stability of uric acid binding to the TAK1-TAB1 complex is further enhanced through the formation of cooperative π–π interactions and the assistance of water molecules that form a bridge between uric acid and protein residues in the binding site (Fig. 5b). Confirming the MD simulation findings, our in vitro kinase assay showed that TAK1 kinase activity is induced by MSU (1, 5, 10, and 50 µg per reaction) in a dose-dependent manner, and TAK1 kinase activity was increased by almost 10-fold by 10 µg MSU when compared to the control values (Fig. 5c; *p* < 0.05).

Furthermore, all ubiquitinated proteins were immunoprecipitated with anti-FK2 antibody and probed for K⁶³-linked ubiquitination. 5Z-7-oxozeaenol treatment, alone or in combination with MSU, restored global K⁶³-linked ubiquitination (Fig. 5d). However, immunoprecipitation of TAK1 and subsequent Western blot analysis showed that 5Z-7-oxozeaenol effectively inhibited the constitutive and MSU-induced K⁶³-linked ubiquitination of TAK1 in THP-1 macrophages (Fig. 5e).

IRAK1, TRAF6, and TAK1 form an activation complex essential for activating the downstream MAPK and NF-κB pathways.^{8,10,26} In

our studies, MSU markedly enhanced the association of IRAK1/TRAF6/TAK1 as an activation complex (Fig. 5f). Interestingly, 5Z-7-oxozeaenol significantly inhibited the ability of TRAF6 to associate with IRAK1 (Fig. 5f, g; *p* < 0.05). These findings provide evidence that 5Z-7-oxozeaenol also reduces the ability of TRAF6 to associate with IRAK1 and disrupts the formation of an activation complex, which is essential for TAK1 activation.^{12,27} These effects result in the marked inhibition in MAPK activation and NF-κBp65 and p-c-Jun nuclear translocation (Fig. 57A, B).

5Z-7-oxozeaenol suppresses MSU-induced paw inflammation. We evaluated the therapeutic potential of targeting TAK1 in a mouse model of MSU-induced inflammation.²¹ The injection of MSU (0.5 mg/20 µl) near the metatarsal joint resulted in paw swelling within 24 h, which resolved after ~96 h (Fig. 58). Based on these findings, mice injected with MSU served as the experimental control and were compared to groups of mice administered 5Z-7-oxozeaenol (5 or 15 mg/kg, per os (p.o.)) 2 h prior to MSU injection (Fig. 6a). Interestingly, 5Z-7-oxozeaenol at 5 and 15 mg/kg markedly inhibited MSU-induced paw inflammation. Histological analysis showed that MSU injection induced the massive infiltration of inflammatory cells, as indicated by a significant increase in the inflammation score, which was inhibited upon 5Z-7-oxozeaenol or febxostat treatment (Fig. 6b; *p* < 0.01). Histopathological evaluation of joints and periarticular connective tissue using H&E staining showed extensive acute and chronic inflammation of the joints and periarticular connective tissue, with associated severe synovitis, erosion of articular cartilage, loss of subchondral bone, pannus formation, and fibrous ankylosis. In contrast, treatment with 5Z-7-oxozeaenol or febxostat

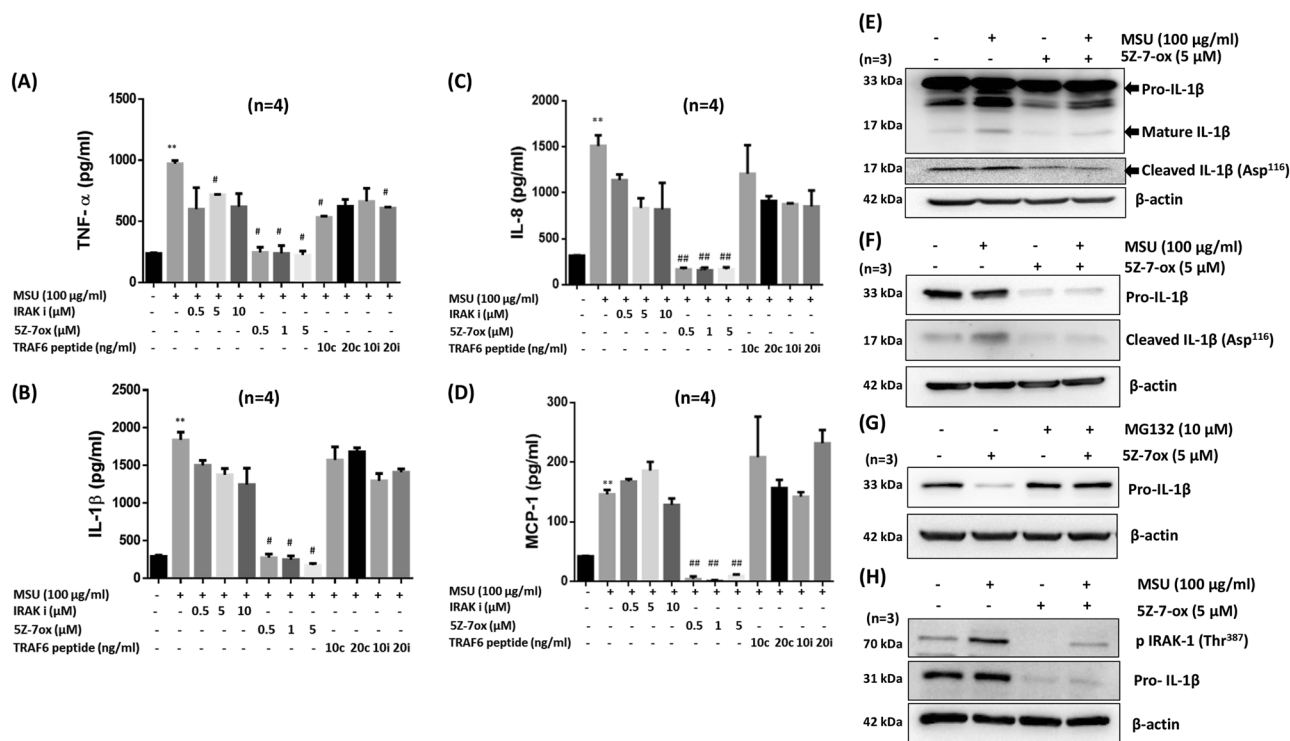


Fig. 4 5Z-7-oxozeaenol selectively inhibits MSU-induced IL-1β, TNF-α, IL-8, and MCP-1 production and reduces expression of the proform of IL-1β and mature IL-1β in THP-1 macrophages. To study the effect of IRAK1, TRAF6, and TAK1 inhibitors on MSU-induced cytokine and chemokine production, THP-1 macrophages were pretreated with an inhibitor of IRAK1 [*N*-(2-morpholinylethyl)-2-(3-nitrobenzoylamido)-benzimidazole, 0.5–10 μM], an inhibitor of TAK1 [5Z-7-oxozeaenol, 5Z-7-ox; 0.05–5 μM], a TRAF6 inhibitor (i) peptide [10–20 μM] or control (c) peptide, [10–20 μM] for 2 h, followed by MSU (100 μg/ml) stimulation for 24 h. Conditioned media were used to estimate the levels of **a** IL-1β, **b** TNF-α, **c** IL-8, and **d** MCP-1 production by ELISA. **e–g** THP-1 macrophages treated with MSU and/or 5Z-7-ox for **e** 30 min or **f** 4 h were lysed, and cell lysates were probed for the proform of IL-1β, mature IL-1β, or cleaved IL-1β (Asp¹¹⁶) by Western blotting. **g** Effect of MG132 on 5Z-7-ox-induced pro-IL-1β degradation. **h** Primary human macrophages were pretreated with 5Z-7-ox, followed by MSU (100 μg/ml) stimulation for 30 min. Cell lysates were probed for p-IRAK1 (Thr³⁸⁷) and pro-IL-1β expression. ***p* < 0.01 for NS (not significant) vs. MSU alone; #*p* < 0.05 or ##*p* < 0.01 for MSU vs. inhibitors

significantly abrogated all the features of acute and chronic inflammation induced by MSU (Fig. 6c; Supplementary Table 1). Western blot analysis of joint homogenates showed that MSU crystals can induce the phosphorylation of TAK1 (Thr^{184/187}) in vivo, which was significantly inhibited by 5Z-7-oxozeaenol treatment (Fig. 6d). Furthermore, MSU crystals markedly induced global K⁴⁸-linked polyubiquitination in vivo, which was markedly reduced by 5Z-7-oxozeaenol (Fig. 6e).

DISCUSSION

This study sheds light on the previously undescribed role of TAK1 and PTMs in mediating MSU-induced inflammation. In particular, we identified that MSU facilitates IRAK1/TAK1/TRAF6 complex formation by activating the K⁶³-polyubiquitination of TAK1 and occupying its binding pocket to induce TAK1 kinase activity. The inhibition of MSU-induced cytokine/chemokine production by 5Z-7-oxozeaenol suggests that TAK1 can serve as a therapeutic target to suppress MSU-induced inflammatory conditions, such as gout.

Studies so far have focused on the downstream events triggered by MSU crystals, with special attention to IL-1β production and its therapeutic regulation.^{2,28} While some studies have pointed at the role of MyD88 and TLR2 in MSU-activated inflammation, we provide evidence that MSU can exploit the ubiquitin proteasome system to relay IL-1β-like inflammatory signals and intensify inflammation. In particular, the temporal activation of IRAK1 by MSU allows the relay of constant cellular signals, thereby permitting association with the E3 ligase TRAF6

and the prolonged activation of downstream TAK1, which controls the MAPK and NF-κB pathways in macrophages and synovial fibroblasts. In addition, the finding that only 5Z-7-oxozeaenol among the signaling inhibitors tested can shut down MSU-induced IL-1β, TNF-α, IL-8, and MCP-1 production suggest TAK1 as a target for gout. While the observed differences in cytokine/chemokine inhibition by small-molecule inhibitors vs. siRNA are open to interpretation, this divergence may be attributed to protein–protein interactions.²⁹ Proteins treated with a small-molecule inhibitor may still act as scaffolds for protein–protein interactions, whereas the treatment of siRNAs with a small-molecule inhibitor can disrupt their biological function and activity. Therefore, the ability of small molecules to target kinase activity without affecting stoichiometry make them a powerful tool for regulating the pathological role of kinases in inflammatory conditions. However, further rigorous experiments related to the dose efficacy and target specificity of TAK1 inhibitors are essential to validate the pharmacological effects identified in this study.

The ubiquitin protein system is responsible for a well-described PTM in cytokine and TLR signaling molecules; however, the means by which MSU crystals exploit this mechanism remain unknown. K⁴⁸-linked proteins are primed for 26s proteasomal degradation, while K⁶³-linked proteins are rescued from 26s proteasome degradation, facilitating stable signal transduction and cellular trafficking.⁹ Studies also suggest that some deubiquitination enzymes (DUBs) play an important role in removing K⁴⁸-linked polyubiquitin chains from proteins “primed” for degradation, thereby reducing or retarding downstream signaling networks.³⁰

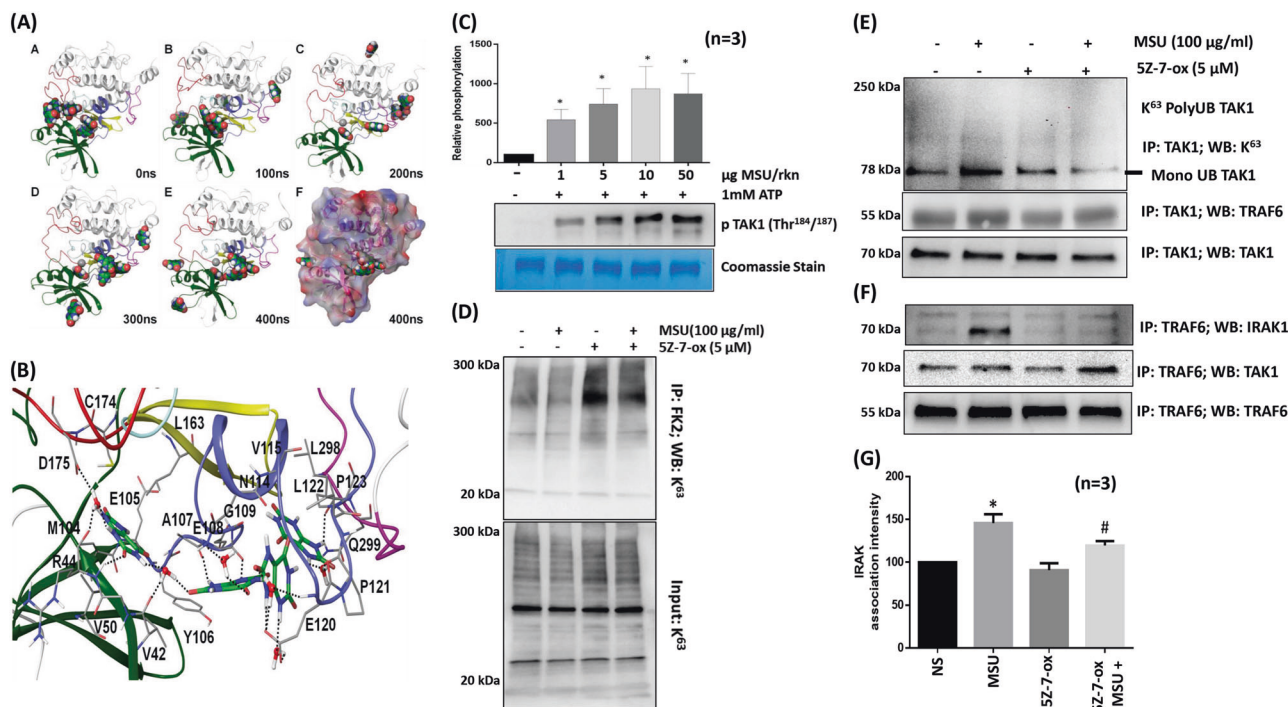


Fig. 5 MSU-induced TAK1 activation and IRAK1/TRAF6/TAK1 complex formation is inhibited by 5Z-7-oxozeaenol. **a** Snapshots of the trajectory of complex formation after every 100 ns; the TAK1-TAB1 fusion protein and six uric acid molecules as ligands were subjected to long 400 ns MD simulation. **b** A representative stable conformation of uric acid molecules in the active site of TAK1, which form a network of H-bonds and hydrophobic interactions with nucleotide-binding residues and engage with D175, which is important for TAK1 autophosphorylation and kinase activity. **c** MSU (1–50 µg) alone or with TAK1-TAB1 recombinant fusion protein was added to THP-1 macrophages to study in vitro kinase activity. Densitometric analysis showed a concentration-dependent increase in TAK1 kinase activity induced by MSU. **d** THP-1 macrophages treated similarly to (Fig. 4e) were immunoprecipitated with an anti-FK2 antibody that recognizes ubiquitin-tagged proteins and probed for K⁶³-linked ubiquitination. **e, f** To determine the effect of 5Z-7-oxozeaenol on IRAK1/TRAF6/TAK1 association, cell lysates from THP-1 macrophages treated with MSU and/or 5Z-7-oxozeaenol were immunoprecipitated with anti-TRAF6 antibody and probed for IRAK1, TAK1, and TRAF6 expression. **g** Densitometric analyses of experiments described in **f** were performed, and the results shown here are the mean ± SEM. Please refer to the Materials and methods section for further details. **p* < 0.05 no ATP vs. TAK1 control; **p* < 0.05 NS (not significant) vs. MSU; #*p* < 0.05 MSU vs. MSU plus 5Z-7-oxozeaenol

Among these DUBs, A20 and CYLD are important in IL-1β and TNF-α signaling and inflammatory regulation,^{31–35} but the role of UCHL2 in cytokine signaling has not yet been studied. Our finding that MSU significantly inhibits A20 and UCHL2 expression in conjunction with increased K⁴⁸-linked ubiquitination suggests that MSU directly upregulates the ubiquitin proteasome system to trigger multicytokine-driven signaling events and inflammasome activity in macrophages. Furthermore, this notion is supported by increased 20s proteasome activity and 26s proteasome subunit PSMD13 expression in MSU-stimulated samples. Importantly, the inhibition of TAK1, which is an important signaling mediator activated by MSU, resulted in the marked inhibition of the release of cytokines and chemokines essential for inflammation.

MSU crystal-induced pathological events have been primarily studied in human monocytes or THP-1-activated macrophages. While some studies have shown the role of MSU in inducing chemokine, nitric oxide and matrix metalloproteinase (MMP) production in synovial fibroblasts or chondrocytes,^{36–38} this is the first study that provides evidence of the role of TAK1 and exploitation of ubiquitination by MSU crystals to cause inflammation. Our findings also provide evidence that MSU can activate TAK1 in human synovial fibroblasts and coordinate with IL-1β at a low concentration to synergistically induce inflammation. Since synovial fibroblasts are a major source of chemokines and MMPs and our recent findings provide evidence of TAK1 as a critical kinase in the IL-1β signaling pathway,¹² these findings suggest that the inhibition of TAK1 significantly impedes the overlapping

MSU-IL-1β signaling networks to downregulate chronic inflammation and tissue destruction.

While several clinical trials have shown the therapeutic efficacy of IL-1 inhibitors such as anakinra and, more recently, rilonacept,^{39–41} others have acknowledged their limitations in the treatment of gout.^{2,7,41} These challenges provide an opportunity to design novel targeted therapeutic approaches to address these limitations and provide ease of delivery as well. While the findings of this study are open to interpretation, we believe that TAK1 inhibitors provide a platform for target validation and drug discovery for the treatment of gout. This belief is further supported by our MD simulation studies, which illustrated the direct interaction of uric acid molecules with the TAK1-TAB1 fusion protein and their ability to stabilize the phosphorylation state of TAK1. This interaction potentially results in sustained downstream signaling that may be the underlying cause of the increased frequency of gouty attacks and accelerated joint destruction.

TAK1 has mostly been ignored due to the fact that TAK1-null mice die at an early embryonic developmental stage.⁴² However, recent studies suggest TAK1 as a therapeutic target in autoimmune diseases governed by IL-1β, such as rheumatoid arthritis, type I diabetes, and multiple sclerosis.^{10,11,43,44} Interestingly, Brown et al.⁴⁵ recently suggested that, unlike other serine threonine kinases, TAK1 possesses a glycine-rich loop positioned opposite the adenosine-binding region of the ATP-binding pocket that exhibits high stoichiometric flexibility (up to 9 Å or 6.6 Å).⁴⁵ This spatial independence allows urate molecules to bind to the TAK1-TAB1 fusion protein and potentially activate TAK1 kinase for

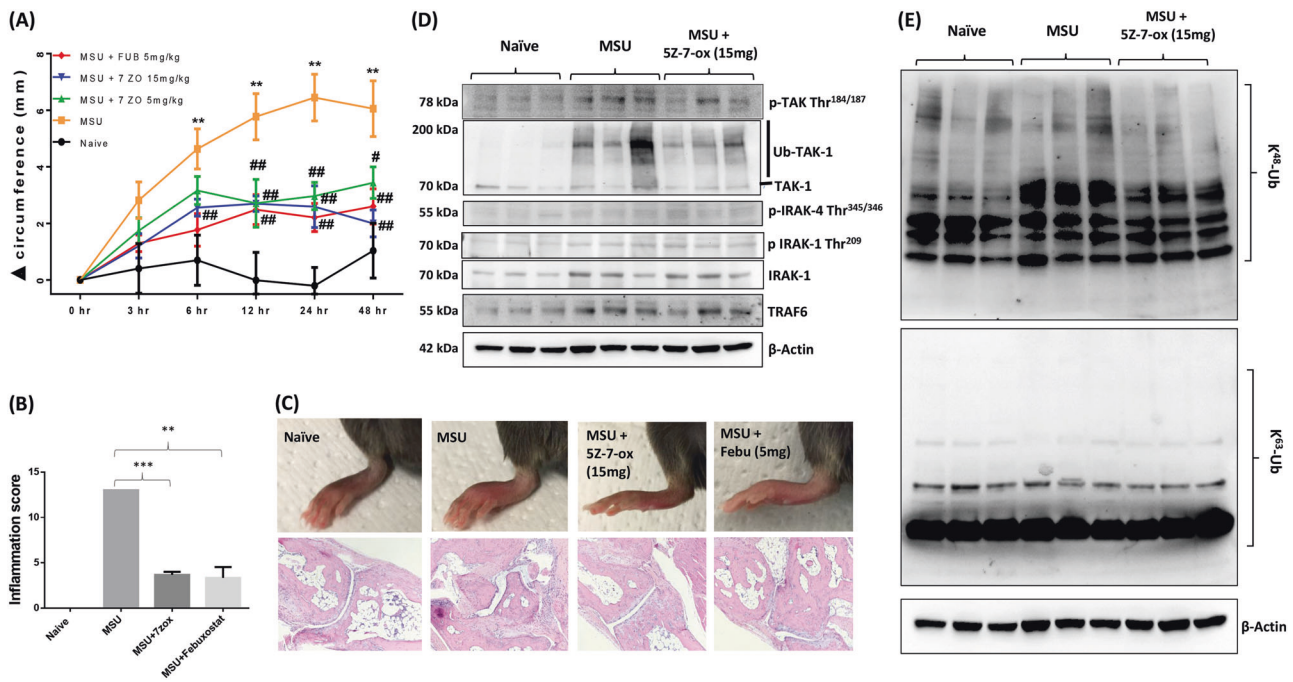


Fig. 6 The TAK1 inhibitor 5Z-7-oxozeaenol suppresses MSU crystal-induced paw inflammation in C57BL6 mice. **a**, MSU (0.5 mg)-induced paw inflammation was measured over 48 h, and the efficacy of 5Z-7-oxozeaenol (5 or 15 mg/kg, p.o.) was evaluated. The change in paw circumference (Δ circumference) was determined and is presented as the mean \pm SEM from $n = 6$ mice per group. **b** A histological analysis of H&E-stained slides was performed by a pathologist blinded to the study to obtain inflammation scores. **c** Representative pictures of treated and untreated ankles (upper panel) and H&E-stained sections (lower panel) from each group are shown. **d** Joint homogenates prepared from naive, MSU-, and MSU plus 5Z-7-ox (15 mg/kg; p.o.)-treated mice were subjected to Western blot analysis for p-TAK1 (Thr^{184/187}), total TAK1, p-IRAK4 (Thr^{345/346}), p-IRAK1 (Thr²⁰⁹), total IRAK1, TRAF6, and β -actin. **e** Western blot analysis of joint homogenates was performed to determine the expression levels of K⁴⁸-linked and K⁶³-linked ubiquitinated proteins. ** $p < 0.01$ or *** $p < 0.001$ for naive vs. MSU alone or MSU vs. treatment; # $p < 0.05$ or ## $p < 0.01$ for MSU v.s 5Z-7-oxozeaenol-treated

a prolonged period, as evidenced by the increased activity of TAK1 in our kinase assay. In addition, the marked inhibition of the MSU-induced synthesis of IL-1 β precursor and its maturation by 5Z-7-oxozeaenol suggests that TAK1 inhibition also transcriptionally suppresses IL-1 β synthesis, thereby limiting its role in inflammation.

Research on targeting IL-1 signaling proteins for therapeutic purposes in inflammatory diseases has gained significant attention, and the targeting of IRAKs has shown some promise.⁴⁶ However, a recent study using IRAK1 knock-in mice showed no effect on the secretion of inflammatory mediators (IL-6, TNF- α , or IL-10), suggesting that IRAK1 catalytic activity is not a rate-limiting step.⁴⁷ Furthermore, the observation that IRAK1-deficient human fibroblasts demonstrate efficient IL-1R-mediated responses⁴⁸ suggests that IRAK1 is not a therapeutic target for crystallopathies. While IRAK1/4 are centrally involved in IL-1 β signaling, other proinflammatory cytokines (TNF- α , RANKL) or TLRs may not rely on IRAKs for effective signal transduction. In contrast, TAK1 plays a crucial role in signaling induced by most of these proinflammatory factors.¹⁰ The results of these studies, taken together with our findings, suggest that TAK1 inhibition has a consistent regulatory impact on MSU-induced inflammation and potentially gout.

Overall, we provide novel insights into the pathogenic effects of MSU crystals on the ubiquitin proteasome system to generate inflammatory responses while highlighting the therapeutic potential of targeting TAK1 to suppress MSU-induced inflammatory events that cannot be regulated by IL-1 inhibitors alone.

ACKNOWLEDGEMENTS

We thank the National Disease Research Interchange, Philadelphia, PA and the Cooperative Human Tissue Network (CHTN), Columbus, OH for providing synovial

tissues. We would also like to thank Sadiq Umar and Bhanupriya Madarampalli for providing technical support in animal experiments. We also thank Ruby Siegel for critical reading of the manuscript. This study was supported by start-up funds from Washington State University.

AUTHOR CONTRIBUTIONS

A.K.S. and S.A. designed this study. A.K.S., K.O.S. and M.H. performed the experiments and participated in drafting the manuscript. S.A. participated in writing the manuscript and provided his support to the study. M.C. participated in writing the manuscript and conducted and analyzed docking and MD simulation experiments. M.O. performed histological analysis and interpreted the results. S.A. is the corresponding author of the manuscript.

ADDITIONAL INFORMATION

The online version of this article (<https://doi.org/10.1038/s41423-019-0284-3>) contains supplementary material.

Competing interests: The authors declare no competing interests.

REFERENCES

- Rees, F., Hui, M. & Doherty, M. Optimizing current treatment of gout. *Nat. Rev. Rheumatol.* **10**, 271–283 (2014).
- So, A. & Busso, N. A magic bullet for gout? *Ann. Rheum. Dis.* **68**, 1517–1519 (2009).
- Chen, C. J. et al. MyD88-dependent IL-1 receptor signaling is essential for gouty inflammation stimulated by monosodium urate crystals. *J. Clin. Invest.* **116**, 2262–2271 (2006).
- Martinon, F., Petrillic, V., Mayor, A., Tardivel, A. & Tschopp, J. Gout-associated uric acid crystals activate the NALP3 inflammasome. *Nature* **440**, 237–241 (2006).
- Martinon, F. & Glimcher, L. H. Gout: new insights into an old disease. *J. Clin. Invest.* **116**, 2073–2075 (2006).
- Bardin, T. Acute inflammatory arthritis: interleukin-1 blockade: a magic wand for gout? *Nat. Rev. Rheumatol.* **5**, 594–596 (2009).

7. Dumusc, A. & So, A. Interleukin-1 as a therapeutic target in gout. *Curr. Opin. Rheumatol.* **27**, 156–163 (2015).
8. Jiang, X. & Chen, Z. J. The role of ubiquitylation in immune defence and pathogen evasion. *Nat. Rev. Immunol.* **12**, 35–48 (2011).
9. Kulathu, Y. & Komander, D. Atypical ubiquitylation—the unexplored world of polyubiquitin beyond Lys48 and Lys63 linkages. *Nat. Rev. Cell. Mol. Biol.* **13**, 508–523 (2012).
10. Fechtner, S., Fox, D. A. & Ahmed, S. Transforming growth factor beta activated kinase 1: a potential therapeutic target for rheumatic diseases. *Rheumatology* **56**, 1060–1068 (2017).
11. Jones, D. S. et al. Profiling drugs for rheumatoid arthritis that inhibit synovial fibroblast activation. *Nat. Chem. Biol.* **13**, 38–45 (2017).
12. Singh, A. K., Umar, S., Riegsecker, S., Chourasia, M. & Ahmed, S. Regulation of transforming growth factor beta-activated kinase activation by epigallocatechin-3-gallate in rheumatoid arthritis synovial fibroblasts: suppression of K(63)-linked autoubiquitination of tumor necrosis factor receptor-associated factor 6. *Arthritis Rheum.* **68**, 347–358 (2016).
13. Bruegel, M., Teupser, D., Haffner, I., Mueller, M. & Thiery, J. Statins reduce macrophage inflammatory protein-1alpha expression in human activated monocytes. *Clin. Exp. Pharm. Physiol.* **33**, 1144–1149 (2006).
14. Pazar, B. et al. Basic calcium phosphate crystals induce monocyte/macrophage IL-1beta secretion through the NLRP3 inflammasome in vitro. *J. Immunol.* **186**, 2495–2502 (2011).
15. Ahmed, S., Pakozdi, A. & Koch, A. E. Regulation of interleukin-1beta-induced chemokine production and matrix metalloproteinase 2 activation by epigallocatechin-3-gallate in rheumatoid arthritis synovial fibroblasts. *Arthritis Rheum.* **54**, 2393–2401 (2006).
16. Akhtar, N., Singh, A. K. & Ahmed, S. MicroRNA-17 suppresses TNF-alpha signaling by interfering with TRAF2 and cIAP2 association in rheumatoid arthritis synovial fibroblasts. *J. Immunol.* **197**, 2219–2228 (2016).
17. Ahmed, S. et al. Epigallocatechin-3-gallate inhibits IL-6 synthesis and suppresses transsignaling by enhancing soluble gp130 production. *Proc. Natl Acad. Sci. USA* **105**, 14692–14697 (2008).
18. Singh, A. K., Fechtner, S., Chourasia, M., Sicalo J. & Ahmed S. Critical role of IL-1alpha in IL-1beta-induced inflammatory responses: cooperation with NF-kappaBp65 in transcriptional regulation. *FASEB J.* <https://doi.org/10.1096/fj201801513R> (2018).
19. Fechtner, S., Singh, A., Chourasia, M. & Ahmed, S. Molecular insights into the differences in anti-inflammatory activities of green tea catechins on IL-1beta signaling in rheumatoid arthritis synovial fibroblasts. *Toxicol. Appl. Pharm.* **329**, 112–120 (2017).
20. Lacey, D. C. et al. Defining GM-CSF- and macrophage-CSF-dependent macrophage responses by in vitro models. *J. Immunol.* **188**, 5752–5765 (2012).
21. Reber, L. L. et al. Contribution of mast cell-derived interleukin-1beta to uric acid crystal-induced acute arthritis in mice. *Arthritis Rheum.* **66**, 2881–2891 (2014).
22. Fechtner, S. et al. Cannabinoid receptor 2 agonist JWH-015 inhibits interleukin-1beta-induced inflammation in rheumatoid arthritis synovial fibroblasts and in adjuvant induced arthritis rat via glucocorticoid receptor. *Front. Immunol.* **10**, 1027 (2019).
23. Wu, J. et al. Mechanism and in vitro pharmacology of TAK1 inhibition by (5Z)-7-oxozeaenol. *ACS Chem. Biol.* **8**, 643–650 (2013).
24. Crisan, T. O. et al. Soluble uric acid primes TLR-induced proinflammatory cytokine production by human primary cells via inhibition of IL-1Ra. *Ann. Rheum. Dis.* **75**, 755–762 (2016).
25. Xiao, J. et al. Soluble monosodium urate, but not its crystal, induces toll like receptor 4-dependent immune activation in renal mesangial cells. *Mol. Immunol.* **66**, 310–318 (2015).
26. Ninomiya-Tsuji, J. et al. The kinase TAK1 can activate the NIK-I kappaB as well as the MAP kinase cascade in the IL-1 signalling pathway. *Nature* **398**, 252–256 (1999).
27. Lamothe, B. et al. Site-specific Lys-63-linked tumor necrosis factor receptor-associated factor 6 auto-ubiquitination is a critical determinant of I kappa B kinase activation. *J. Biol. Chem.* **282**, 4102–4112 (2007).
28. Edwards, N. L. & So, A. Emerging therapies for gout. *Rheum. Dis. Clin. N. Am.* **40**, 375–387 (2014).
29. Weiss, W. A., Taylor, S. S. & Shokat, K. M. Recognizing and exploiting differences between RNAi and small-molecule inhibitors. *Nat. Chem. Biol.* **3**, 739–744 (2007).
30. Mevissen, T. E. T. & Komander, D. Mechanisms of deubiquitinase specificity and regulation. *Annu. Rev. Biochem.* **86**, 159–192 (2017).
31. Chen, Z. J. Ubiquitination in signaling to and activation of IKK. *Immunol. Rev.* **246**, 95–106 (2012).
32. Duong, B. H. et al. A20 restricts ubiquitination of pro-interleukin-1beta protein complexes and suppresses NLRP3 inflammasome activity. *Immunity* **42**, 55–67 (2015).
33. Lork, M., Verhelst, K. & Beyaert, R. CYLD, A20 and OTULIN deubiquitinases in NF-kappaB signaling and cell death: so similar, yet so different. *Cell Death Differ.* **24**, 1172–1183 (2017).
34. Shembade, N., Ma, A. & Harhaj, E. W. Inhibition of NF-kappaB signaling by A20 through disruption of ubiquitin enzyme complexes. *Science* **327**, 1135–1139 (2010).
35. Skaug, B. et al. Direct, noncatalytic mechanism of IKK inhibition by A20. *Mol. Cell* **44**, 559–571 (2011).
36. Liu, R., Liote, F., Rose, D. M., Merz, D. & Terkeltaub, R. Proline-rich tyrosine kinase 2 and Src kinase signaling transduce monosodium urate crystal-induced nitric oxide production and matrix metalloproteinase 3 expression in chondrocytes. *Arthritis Rheum.* **50**, 247–258 (2004).
37. Liu-Bryan, R., Pritzker, K., Firestein, G. S. & Terkeltaub, R. TLR2 signaling in chondrocytes drives calcium pyrophosphate dihydrate and monosodium urate crystal-induced nitric oxide generation. *J. Immunol.* **174**, 5016–5023 (2005).
38. Zheng, S. C. et al. Role of the NLRP3 inflammasome in the transient release of IL-1beta induced by monosodium urate crystals in human fibroblast-like synoviocytes. *J. Inflamm.* **12**, 30 (2015).
39. Baldwin, A. G., Brough, D. & Freeman, S. Inhibiting the inflammasome: a chemical perspective. *J. Med. Chem.* **59**, 1691–1710 (2016).
40. Cavalli, G. & Dinarello, C. A. Treating rheumatological diseases and co-morbidities with interleukin-1 blocking therapies. *Rheumatology* **54**, 2134–2144 (2015).
41. Davies, K. & Bukhari, M. A. S. Recent pharmacological advances in the management of gout. *Rheumatology* <https://doi.org/10.1093/rheumatology/kex343> (2017).
42. Sato, S. et al. Essential function for the kinase TAK1 in innate and adaptive immune responses. *Nat. Immunol.* **6**, 1087–1095 (2005).
43. Cao, H. et al. TAK1 inhibition prevents the development of autoimmune diabetes in NOD mice. *Sci. Rep.* **5**, 14593 (2015).
44. Xiao, Y. et al. TPL2 mediates autoimmune inflammation through activation of the TAK1 axis of IL-17 signaling. *J. Exp. Med.* **211**, 1689–1702 (2014).
45. Brown, K. et al. Structural basis for the interaction of TAK1 kinase with its activating protein TAB1. *J. Mol. Biol.* **354**, 1013–1020 (2005).
46. Singer, J. W. et al. Inhibition of interleukin-1 receptor-associated kinase 1 (IRAK1) as a therapeutic strategy. *Oncotarget* **9**, 33416–33439 (2018).
47. Pauls, E. et al. Two phases of inflammatory mediator production defined by the study of IRAK2 and IRAK1 knock-in mice. *J. Immunol.* **191**, 2717–2730 (2013).
48. Della Mina, E. et al. Inherited human IRAK-1 deficiency selectively impairs TLR signaling in fibroblasts. *Proc. Natl Acad. Sci. USA* **114**, E514–E523 (2017).